Chemical Engineering Journal Advances 14 (2023) 100472

Contents lists available at ScienceDirect

Chemical Engineering Journal Advances

journal homepage: www.sciencedirect.com/journal/chemical-engineering-journal-advances

Heat-activated peroxydisulfate and peroxymonosulfate-mediated degradation of benzotriazole: Effects of chloride on kinetics, pathways and transformation product toxicity

Pradip Saha [a,b], Chenyu Zhou [a], Mahsa Moradi [a,c], Huub H.M. Rijnaarts [a], Harry Bruning [a,*]

[a] Department of Environmental Technology, Wageningen University and Research, PO Box 17, 6700 AA Wageningen, The Netherlands
[b] Department of Chemical Engineering and Polymer Science, Shahjalal University of Science and Technology, Sylhet 3114, Bangladesh
[c] Department of Environmental Health Engineering, School of Public Health, Tehran University of Medical Sciences, Tehran, Iran

ARTICLE INFO

Keywords:
Benzotriazole
Heat-activated peroxydisulfate/ peroxymonosulfate
Chloride
Chlorinated by-products
Toxicity

ABSTRACT

The impact of chloride (Cl^-) in heat-activated peroxydisulfate (PDS) and peroxymonosulfate (PMS) processes for benzotriazole (BTA) degradation was investigated. Results showed that 0.42 mM BTA could be degraded by PDS and PMS under 70 °C in presence and absence of Cl^-. The PMS-mediated BTA degradation rate increased with increasing Cl^- concentration up to 1000 mg/L, while a further increase of Cl^- concentration decreased the BTA degradation rate. In contrast, Cl^- inhibited PDS-mediated BTA degradation at concentrations tested between 100 and 10,000 mg/L. Radical scavenging experiments indicated that BTA degradation was mainly driven by hydroxyl and sulfate radicals in PDS and PMS systems without Cl^-. However, reactive chlorine species (RCS) significantly boosted the PMS system for BTA degradation in presence of Cl^-. Variation in pH substantially influenced the PMS system, but not the PDS system, whether in presence and absence of Cl^-. By LC-MS/MS analysis, forty-two transformation products (TPs) were identified resulting from BTA degradation. Based on the TPs, polymerization, hydroxylation, benzene ring-opening, and carboxylic acid formation were hypothesized to be the main degradation mechanisms in absence of Cl^-, whereas chlorination, triazole ring-opening, and nitration were the additional degradation steps in presence of Cl^-. These findings help understand the influence of Cl^- on BTA removal rate and degradation pathway in saline wastewater. Moreover, more chlorinated TPs were found in PMS/Cl^- system than in PDS/Cl^- system, which was also reflected in absorbable organic halides (AOX) and end-product toxicity analyses. The PMS/Cl^- process also produced other undesirable by-products, such as chlorates which were not detected in the PDS/Cl^- process. This shows that PDS and PMS-based advanced oxidation processes can notably differ in terms of toxic by-product formation. Thus, they need to be critically evaluated before applying for organic pollutant degradation under saline conditions.

1. Introduction

As a chemical with high consumption within industries, benzotriazole (BTA) is mentioned in the NORMAN network list of emerging pollutants [1] and the Dutch River Water Companies Association (RIWA) list of potential pollutants (Dutch watchlist) [2]. Indeed, BTA is extensively used in industries and is a constituent of many chemical products such as corrosion inhibitors, anti-icing fluids, pharmaceuticals, textile dyes, plastics and rubbers, and dishwashing formulas [3,4]. Due to its high water solubility, low partition coefficient (K_{ow}), poor biodegradability, and incomplete removal in conventional wastewater treatment plants especially within industries, BTA is a frequently detected contaminant in water bodies [5–7]. In a study conducted by Seeland et al., it was reported that 7 to 100 μg/L BTA was detected in European surface waters, and its concentration reached up to mg/L level in the vicinity of the airports [8]. In cooling tower operation, around 3 to 6 mg/L BTA is usually added to the makeup water [9,10]. Thus, BTA is extensively used within industries while it is not efficiently removed in conventional treatment processes, thereby it shows up within the waterbodies [11]. Besides, BTA can accumulate in the environment and is a carcinogenic and mutagenic compound [12,13]. Therefore, developing an effective treatment method for BTA removal is essential.

Regarding the poor biodegradability of BTA, advanced oxidation is an interesting candidate for its treatment. Different advanced oxidation

* Corresponding author.
E-mail address: harry.bruning@wur.nl (H. Bruning).

https://doi.org/10.1016/j.ceja.2023.100472

Available online 23 February 2023

processes (AOPs) have been studied for BTA degradation, such as photoelectrochemical and photocatalytic processes, Fenton-processes, photolysis, vacuum UV, ozonation, and sulfate radical ($SO_4^{\bullet-}$)-based processes (SR-AOPs) [14–24]. SR-AOPs have become more interesting for the degradation of recalcitrant organic compounds, like BTA, since $SO_4^{\bullet-}$ has a high oxidation potential, a longer lifetime, and higher stability at a wide pH range as compared to $HO^{\bullet}$ [25–27]. $SO_4^{\bullet-}$ can be formed from specific precursors, e.g., peroxydisulfate (PDS) and peroxymonosulfate (PMS) activation, facilitated by heat, light (sunlight or UV), high pH, ultrasound, H_2O_2, activated carbon catalyst, electrochemical process, and different transition metals/metal oxides. Indeed, persulfate activation enhances PMS and PDS oxidizing capacity via radical and non-radical degradative reaction routes [28]. Several studies show that SR-AOPs effectively remove BTA from aqueous environments [4,17,21,29–31]. However, transformation products (TPs) and the fate of chloride ions (Cl^-), often present in the water matrix, still need to be examined critically in BTA degradation in SR-AOPs, for the reason that toxic reaction products can be formed.

Chloride (Cl^-) is present in aquatic environments with a concentration range of 0.001 M to 1 M [32]. Several studies have reported that Cl^- might react with $HO^{\bullet}$ and $SO_4^{\bullet-}$, forming less effective chlorine radicals ($Cl^{\bullet}$), which may further be converted to $Cl_2^{\bullet-}$ [33,34]. Besides, Cl^- may directly react with PMS to produce free chlorine (Cl_2/HOCl/ClO^-)[28]. Thus, Cl^- introduces reactive chlorine species or RCS ($Cl^{\bullet}$, $Cl_2^{\bullet-}$, and Cl_2/HOCl/ClO^-) in the system, influencing the BTA degradation kinetics, pathways, and TPs distribution.

In a study conducted by Lei et al., PMS and PMS/Cl^- systems were studied and compared for the degradation of Rhodamine B (RhB) [35]. It was found that Cl^- could accelerate the degradation of RhB through formation of free available chlorine species. However, degradation intermediates were not monitored within the system. Hence, the authors recommended reinvestigation of PMS and Cl^- roles in PMS-based AOPs in future works [35]. One study showed that BTA degradation efficiency by heat-activated PDS was enhanced when low concentrations of Cl^- (<10 mM) were added, while higher concentrations of Cl^-hindered the degradation [21]. However, in the (Cobalt)Co-activated PMS system, phenol and dye degradation efficiencies decreased when the Cl^- concentration was below 5 mM and increased above 50 mM [36–38]. The 4-chlorophenol degradation rate increased by 47 times during the UV-activated PMS process in the presence of high Cl^- concentration [39]. Apart from RCS reactivity with the reactive oxygen species, its reactivity with the organic compounds is also critical in determining the effect of Cl^- in such systems. The reaction between organic compounds and RCS may form chlorinated TPs in the form of absorbable organic halides (AOX). Potentially, AOX is more toxic and refractory than the parent organic compounds. Based on the previous studies, chlorinated TPs are formed during the degradation of monochlorophenols, bezafibrate, and carbamazepine in UV-activated PDS in presence of Cl^- [34, 40]. Similarly, a substantial amount of chlorinated TPs was reported during the degradation of steroid estrogens, methylene blue, 4-chlorophenol, phthalic acid, 2,4,6-trichlorophenol, and phenol in SR-AOPs in presence of Cl^-. Even though several TPs were reported during BTA degradation by SR-AOPs, the evaluation of chlorinated TPs formation and the corresponding degradation pathway still need to be elucidated [18,22,41,42].

Moreover, research shows that chlorate (ClO_3^-) is produced during the SR-AOPs in presence of Cl^- [43]. A study reported that all Cl^- was converted to ClO_3^- before the degradation of perfluorooctanoic acid in the UV-activated PDS system [44]. Another research shows that ClO_3^- has been formed in the UV-activated PDS and Co-activated PMS systems, and the formation rate depends on the Cl^- concentration [45]. The acidic pH was more favorable for ClO_3^- formation in a UV-activated PDS process [41]. Due to the toxicity, the world health organization [46] advises keeping the ClO_3^- concentration less than 0.7 mg/L in the drinking water [46]. The US-EPA and Switzerland authorities also recommend keeping the ClO_3^- level below 200–210 μg/L in drinking water during UV-activated PDS treatment [45]. Thus, the formation of ClO_3^- during the BTA degradation in SR-AOPs is essential to monitor.

Therefore, the primary focus of this study was deep assessment of the influence of Cl^- in BTA degradation using heat-activated PDS and PMS systems. For this purpose, BTA samples were synthetically prepared with temperature similar to that of a typical cooling tower blowdown. Hence, heat (70 °C) was selected as both PDS and PMS activator due to its simplicity, moderate reaction conditions, no addition of chemicals/catalyst [47], and beneficial use of waste heat. Indeed, waste heat from industries, for instance, cooling towers can be used for PDS and PMS activation [9,48,49]. The roles and dominance of important radicals in BTA degradation were investigated with scavenging experiments. TPs were identified by using LC-MS/MS to see their distribution and speciation in presence and absence of Cl^-. Last but not least, AOX, ClO^-, and ClO_3^-accumulation, acute toxicity, and BTA mineralization were explored under different experimental conditions. Recommendations are given for PDS and PMS process selection to avoid toxic products forming.

2. Materials and methods

2.1. Chemicals

1-H benzotriazole (BTA, $C_6H_5N_3$, 99%; Table S1) and ammonium formate (HCO_2NH_4, HPLC grade) were purchased from Sigma Aldrich Chemie B·V (the Netherlands). Sodium peroxydisulfate (PDS, $Na_2S_2O_8$, 99%), potassium peroxymonosulfate (PMS, $2KHSO_5{\cdot}KHSO_4{\cdot}K_2SO_4$, 99%), sodium chloride (NaCl, 99%), sodium dihydrogen phosphate (NaH_2PO_4, 99%), sodium hydrogen phosphate (Na_2HPO_4, 99%), Sulfuric acid (H_2SO_4, 95–98%), tert-butyl alcohol (TBA, C_4H_9OH, 99%), sodium hydroxide (NaOH, 99%) ethanol (EtOH, 99%), N,N-diethyl-p-phenylenediamine (DPD, 99%), L-Histidine ($C_6H_9N_3O_2$, ≥99%), and sodium azide (NaN_3, 99.5%) were obtained from Merck Chemicals B.V. (the Netherlands). Methanol ultra (MA, CH_3OH) was obtained from LPS b.v. (the Netherlands) and Formic acid (CH_2O_2, ULC/MS) was purchased from Biosolve BV, the Netherlands. All the experiments were conducted using Millipore Milli-Q® water purification (electrical resistivity 18.6 MΩ; Millipore Corporation, USA).

2.2. Experimental procedures

The experiments were conducted in 150 mL glass bottles equipped with an online pH meter (Prosense, Oosterhout, the Netherlands). The bottles were filled with 0.42 mM BTA, different concentrations of Cl^- (0, 100, 1000, and 10,000 mg/L), and 15 mM phosphate buffers unless otherwise mentioned. The bottles were preheated for 30 min in a shaking water bath oscillating at 150 rpm (SW23, JULABO GmbH, Germany), and 15 mM PDS or PMS was added. Pre-tests showed that when PDS or PMS was added to the bottles, the pH decreased quickly, even in presence of buffer. Thus, the pH was adjusted by 6 M NaOH to the desired value during the experiment. At specific time intervals, samples were collected and put in an ice bath to quench the reaction immediately. BTA, free chlorine, and PDS or PMS concentrations were measured the same day the sample was taken to rule out storage influence. For TOC, AOX, and ClO_3^- analyses, samples were stored at -20 °C and measured the following day after the experiment. Experiments were carried out without phosphate buffer for TPs identification to avoid buffers' effects on the TPs formation. A certain amount of EtOH or TBA was added to the bottles as a scavenger for $HO^{\bullet}$ and $SO_4^{\bullet-}$, respectively [50,51]. L-Histidine and sodium azide were added to the bottles as singlet oxygen ($^1O_2$) scavengers. Control experiments with BTA without PDS or PMS at 70 °C showed that BTA was hydrolysis-resistant and thermally stable. Control experiments of BTA degradation with PDS or PMS at 25 °C were carried out (Fig. S1).

2.3. Analytical methods

A Thermo Scientific HPLC quantified the BTA concentration with a fluorescence detector at 278 nm. The separation was performed by a Phenyl-Hexyl column (ACQUITY UPLC, 1.7 μm, 2.1 × 150 mm). The mobile phases were (A): water/formic acid 0.01% (v/v) and (B): acetonitrile/formic acid 0.01% (v/v) with a 0.2 mL/min flow rate. The injection volume was 10 μL, and the column temperature was 35 °C. TOC was determined by a total organic carbon analyzer TOC-L CPH/CPN system integrated with ASI-L autosampler (Shimadzu, Benelux) using a Non-Purgeable Organic Carbon (NPOC) method. The PDS/PMS concentration was determined by a spectrophotometric method combined with 0.1 mL of 2.5 mM N, N-diethyl-p-phenylenediamine (DPD) at 510 and 551 nm [52]. The ion chromatograph model, ICS 2100 with Dionex (IonPac AG17 Guard 4 × 50 mm and IonPac AS17 analytical 4 × 250 mm column), was used for measuring the concentration of ClO_3^-. AOX was determined by LCK 930 Hach Dr. Lange cuvette test kits using a Hach DR./3900 spectrophotometer (Hach Lange GmbH, Germany). Marine luminescent *Vibrio Fischeri* bacteria were used to assess the acute toxicity of BTA and its TPs [53]. The inhibition effect of untreated samples was also measured as a control. The free chlorine (FC) concentration was measured with the DPD–FAS standard method [54]. PDS and PMS interfered with the free chlorine measurement; thus, a modification was introduced according to [55] to the standard method. Phosphate buffer and DPD solution were prepared according to the standard DPD–FAS method. 5 ml buffer was mixed with 5 ml of DPD solution; 20 mL of 5% EDTA was added to the mixture. Finally, a 50 mL sample was mixed and titrated with ferrous ammonium sulfate (FAS). 1 mL of FAS is equivalent to 0.1 mg Cl_2.

2.4. High-resolution LC-MS/MS analysis for TPs identification

The TPs were analyzed by Ultimate 3000 liquid chromatography coupled with a QExactive Orbitrap MS- a high-resolution accurate- mass spectrometer (Thermo Scientific, San Jose, CA, USA). 50 μL injected sample was separated in an Atlantis T3 column (100 mm × 3 mm, 3 μm) with 0.3 mL/min eluant flow for 20 min. Eluant consisted of solution (A): Water/2 mM ammonium formate/0.016% (v/v) formic acid and (B): methanol/2 mM ammonium formate /0.016% (v/v) formic acid. The elution gradient was 0% B initially, which linearly increased to 45% in 2 min, subsequently increased to 100% in 8 min, and was kept constant up to 14.5 min. In the next 0.5 min, B decreased to 0%, and this condition was maintained until 20 min. The column oven temperature was 40 °C, and TPs were detected in full-scan mode (60–700) in both positive and negative ionization modes. During the measurement, MS was at 3.5 kV spray voltage; 48 sheaths and 2 (a.u.) sweep gas flow; 256 °C capillary temperature; 413 °C aux gas heater temperature and 70,000 resolution power. According to the manufacturer protocol, MS was calibrated for each series using a Pierce™ LTQ Velos ESI positive and negative ion calibration solution (Thermo Scientific).

2.5. Data analysis

2.5.1. Data processing for TPs identification

LC-MS raw data files obtained from duplicate measurements were processed by commercially available small molecule structure identification software "Compound Discoverer (CD) v. 3.1" (Thermo Scientific, USA). The environmental workflow template "Environmental w Stats Unknown ID w Online and Local Database Searches" was used. The workflow consists of five general steps: (1) raw files are inputted in the CD and named as samples or blank; (2) spectra of peaks are picked based on minimum peak intensity counts (100,000 a.u), mass tolerance (5 ppm), and retention time shift (0.2 min); (3) the compounds are detected based on mass tolerance, intensity threshold, isotopes integration and ions adducts from extracted ion chromatogram (XIC) traces in the full scans (MS1). Compounds with the same molecular weight and retention time were grouped together; (4) in the predict compositions step, the molecular formula is assigned according to the accurate mass, maximum element counts "$C_{90}H_{190}Cl_{10}N_{10}O_{15}S_5$"; (5) best-fit compounds are selected based on composition and mass from ChemSpider and mass lists database search. The matching results are further filtered and checked based on peak shape, peak area, and relevance to the parent compound to make the results more reliable.

2.5.2. Scavengers effect calculation

The percentage decrease in reaction rate constant k_{obs} (PDS/PMS) due to scavengers was calculated by the following formula (Eq. (1)):

$$\%\text{decrease of } k_{obs}(D\%) = \left[1 - k_{obs(\text{scavenger})} \,/\, k_{obs(\text{without scavengers})}\right] \times 100\% \quad (1)$$

2.5.3. Toxicity calculation

The increase of luminescent intensity inhibition was used to evaluate the toxicity and calculated as follows (Eq. (2)):

$$\text{Increase of inhibition}(\%) = \frac{L_0 - L}{L} \times 100\% \quad (2)$$

L_0 is the luminescent intensity of the control sample (before reaction), and L is the luminescent intensity of a sample.

3. Results and discussion

3.1. BTA degradation kinetics in the absence and presence of Cl^-

The effect of 0, 100, 1000, and 10,000 mg/L Cl^- on BTA degradation in heat-activated PDS and PMS was investigated and shown in Fig. 1.

The Cl^- concentration significantly influenced the BTA degradation in both PDS and PMS systems but in different ways (Fig. 1). Fig. 1a shows that BTA degradation was retarded in the PDS/Cl^- process. In the absence of Cl^-, the pseudo-first-order rate constant (k_{obs}) for BTA degradation was 0.07 min^{-1}. This value was lowered to 0.05 min^{-1} when the Cl^- concentration was increased to 100 mg/L. Further increasing the Cl^- concentration to 10,000 mg/L led to a continued decrease of the k_{obs} to 0.03 min^{-1}. The BTA removal efficiency was also reduced to 96% in 10,000 mg/L Cl^- after 120 min of reaction time. Cl^- can react with $SO_4^{\bullet-}$ to produce $Cl^{\bullet}$ with a rate constant of 3.2 × 10^8 min^{-1}, pushing back to $SO_4^{\bullet-}$ with a rate constant of the reversed reaction of 2.1 × 10^8 min^{-1} (Eq. (3)).

$$SO_4^{\bullet-} + Cl^- \leftrightarrow SO_4^{2-} + Cl^{\bullet} \quad (3)$$

$SO_4^{\bullet-}$ has supposedly been produced again, compensating the $SO_4^{\bullet-}$ scavenging at low Cl^- concentration [56–58]. Thus, low Cl^- concentration lowers the BTA degradation rate slightly. However, when Cl^- was at an elevated concentration (10,000 mg/L), the forward reaction became dominant, resulting in a higher degree of $SO_4^{\bullet-}$ scavenging. Thus, the overall BTA k_{obs} and efficiency decreased with increasing Cl^- concentration. The BTA degradation was promoted remarkably in the PMS/Cl^- process (Fig. 1b). The increase of Cl^- concentration increased the BTA k_{obs} up to 1000 mg/L Cl^-. In the absence of chloride, the k_{obs} was 0.03 min^{-1}. Adding 100 mg/L and 1000 mg/L Cl^- led to a notable increase of k_{obs} to 0.1 min^{-1} (three times higher) and 0.3 min^{-1} (ten times higher), respectively. However, further rising of the Cl^- concentration decreased the rate.

Meanwhile, the BTA removal efficiency after 120 min reaction increased from 95% (without Cl^-) to 100% (100 mg/L, 1000 mg/L and 10,000 mg/L Cl^-). Especially when Cl^- was 1000 mg/L, 100% BTA was removed in 20 min. Similar results were obtained in research focused on acid Orange 7 (AO7) degradation by anion activation of PMS, reporting that 10 mM and 100 mM Cl^- could effectively activate the PMS but not the PDS [59]. In a study by Zhang et al. [57], p-aminobenzoic acid degradation efficiency was enhanced by increasing Cl− dosage using

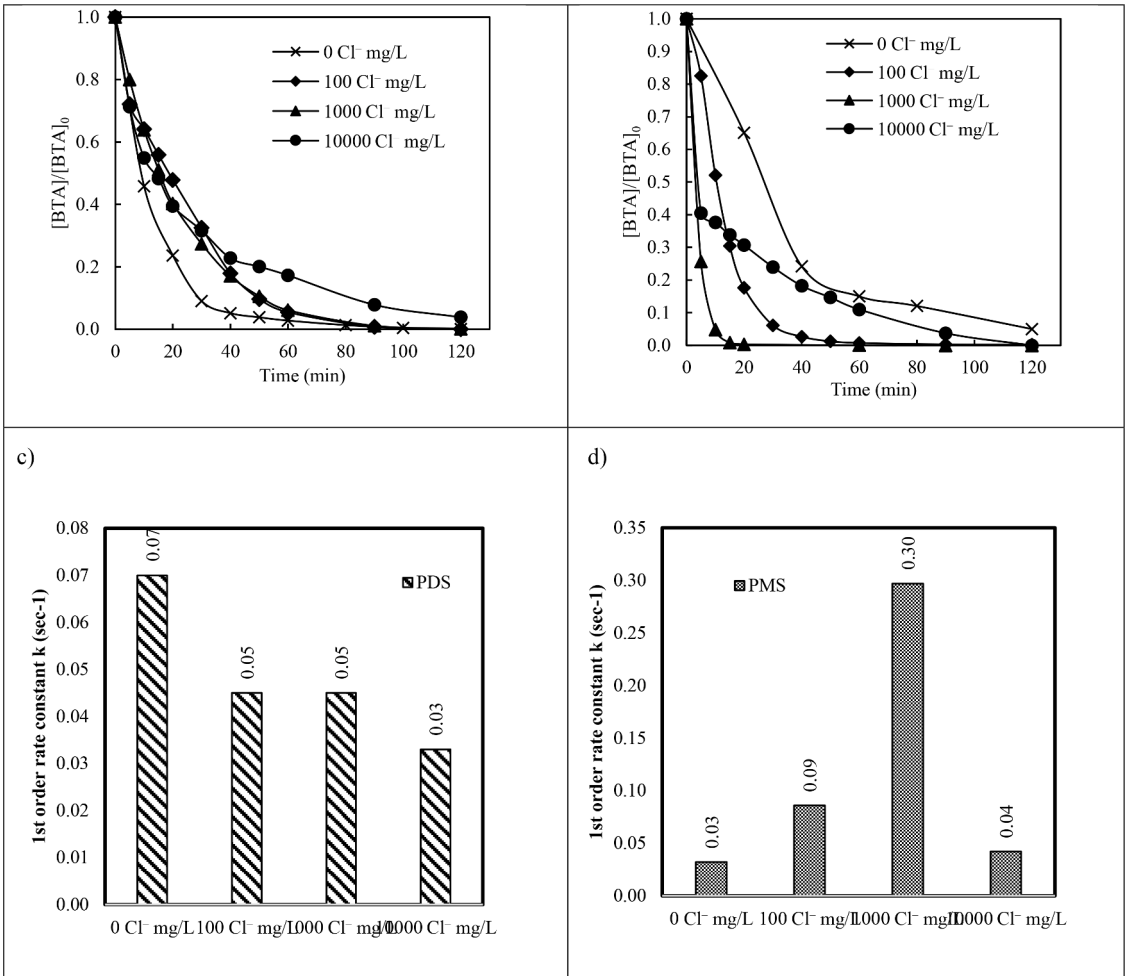

Fig. 1. BTA degradation by (a) PDS and (b) PMS in the presence of 0 mg/L, 100 mg/L, 1000 mg/L and 10,000 mg/L Cl^- during 120 min reaction; (c)& (d) Pseudo-first-order disappearance of BTA for PDS and PMS; Experimental conditions: $T = 70$ °C, $[BTA]_0 = 0.42$ mM, $[PDS]_0 = [PMS]_0 = 15$ mM, $V = 100$ mL, all experiments were buffered by 15 mM phosphate and sodium hydroxide was added dropwise to maintain the pH around 6.8–7.3.

PMS. An increase of chloride up to 200 mM led to complete removal of p-aminobenzoic acid in 20 min; while in the absence of chloride, p-aminobenzoic acid removal efficiency reached merely 81% in reaction time of as long as 80 min. Direct PMS oxidation was identified as the major contributor to p-aminobenzoic acid degradation, while HClO/ClO^- was identified as the dominant RCS [60]. Another study investigated the role of chloride on ammonia oxidation by cobalt-doped graphitic carbon nitride-activated PMS [61]. It was hypothesized that at pH levels higher than 6, free chlorine species mostly react with water leading to the formation of $HO^\bullet$ thereby boosting the oxidation rate

Due to the unsymmetrical structure of PMS, it is easily attacked by a nucleophile such as Cl^- [62]. Yang et al. also showed that PMS could react with Cl^- producing OCl^- [59,63]. Thus, active OCl^- together with $HO^\bullet$ and $SO_4^{\bullet-}$ radicals facilitated the degradation of BTA up to 1000 mg/L Cl^-. Further increasing of Cl^- concentration could quench the radicals and hinder the BTA degradation.

3.2. *pH influence on BTA degradation kinetics in absence and presence of Cl^-*

The BTA degradation in PDS and PMS systems at varying pH is shown in Fig. 2. Fig. 2a indicates that the pH changes barely influenced the BTA k_{obs} in PDS experiments. Complete BTA removal efficiency was obtained under all pH conditions after 120 min reaction. The k_{obs} (PDS) at pH 7 and 11 was 0.07 min^{-1} both in absence of Cl^-, while in presence of 1000 mg/L Cl^-, k_{obs} (PDS) was 0.05 min^{-1}. Some studies indicated that organics degradation could be improved at alkaline conditions as compared to acidic conditions [64]. However, BTA degradation rates were similar at pH 7 and 11, as reported in other studies [65]. Interestingly, it was observed that PDS consumptions at pH = 7 and pH = 11 were 33% and 21%, respectively; after 180 min (Fig. S1). Supposedly, $SO_4^{\bullet-}$ radicals were converted to $HO^\bullet$ at a high rate [66]. $HO^\bullet$ has higher redox potential and is unselective [48]. Thus, alkaline conditions lead to decreased PDS consumption without Cl^-. However, PDS consumption was similar (around 34%) in both pH levels in presence of Cl^- because Cl^- can be a scavenger for $SO_4^{\bullet-}$ and $HO^\bullet$ resulting in the generation of RCS [67,68].

Fig. 2b indicates that the pH significantly affects BTA degradation in the PMS system. At pH = 11, only 70% of BTA was decomposed after 120 min with k_{ob} of 0.02 min^{-1} in the absence of chloride, whereas at pH = 7 in identical conditions, 95% BTA removal efficiency was obtained with k_{ob} of 0.03 min^{-1}. At pH 11, the BTA degradation rate was high in the first 20 min, and then it became extremely low Fig. 2b). From 20 min to 120 min, only 12% of BTA was degraded, whereas 58% of BTA was degraded in the first 20 min. It was reported that SO_5^{2-}, which can be generated at alkaline conditions (Eq. (4)), was more accessible to activate than HSO_5^-, thus, more radicals were produced [69]. This explains the high BTA degradation rate in the first 20 min. However, some PMS were decomposed at pH 11 rather than converting into radicals (Eqs. (5) and (6) [70].

$$HSO_5^- + H_2O \rightleftarrows SO_5^{2-} + H_3O^+ \ (pK_{a2}=9.4) \quad (4)$$

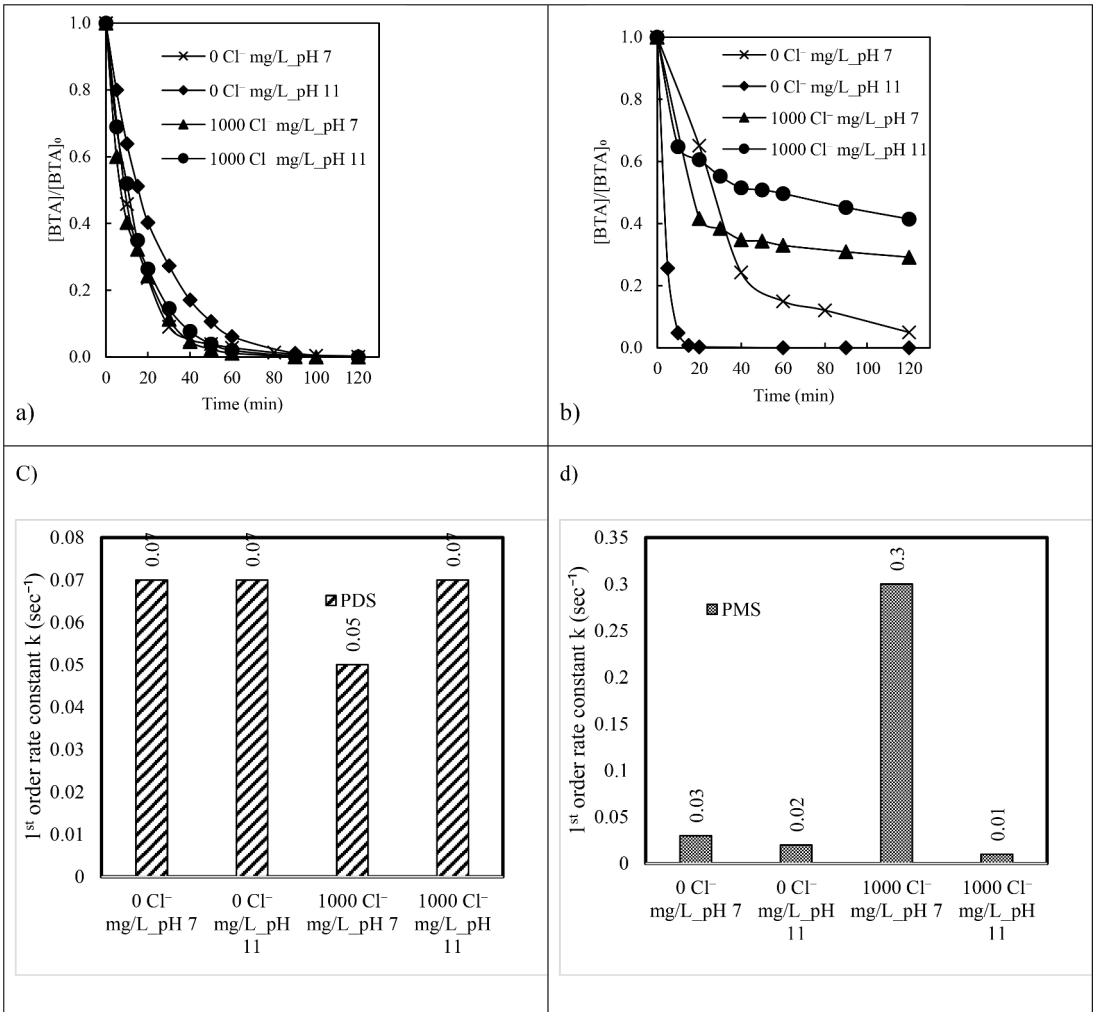

Fig. 2. The effect of pH on BTA degradation by (a) PDS and (b) PMS in absence and presence of Cl^- (1000 mg/L) during 120 min reaction; (c) & (d)Pseudo-first-order disappearance of BTA for PDS and PMS; Experimental conditions: $T = 70$ °C, $[BTA]_0 = 0.42$ mM, $[PDS]_0$=$[PMS]_0 = 15$ mM, $V = 100$ mL.

$$HSO_5^- + SO_5^- \rightarrow \text{the activated complex} \rightarrow HSO_6^- + SO_4^- \quad (5)$$

$$HSO_6^- + OH^- \rightarrow SO_4^{-2} + H_2O + O_2 \quad (6)$$

Yang et al. [71] found that at pH 11, about 75% of PMS was decomposed after 20 min, and 100% of PMS was decomposed after 120 min in the wet scrubbing process. 2 g/L Na_2SiO_3 was used to make the PMS more stable in their experiments [71]. In the current study, no PMS was left at pH 11 and 70 °C in 120 min, but the BTA removal efficiency was only 70%. At 30 min, 82% PMS was consumed (Fig. S1). The residual PMS was only 9%, with 12% BTA removal efficiency in pH 11 at 25 °C after 120 min (Fig. S1). The high PMS consumption rate and low BTA removal efficiency at pH 11 reflected that a large part of PMS was decomposed instead of forming $SO_4^{\bullet-}$ or $HO^{\bullet}$ radicals. Fig. S2 also illustrates the variation trend of PMS concentration (%) over time at 70 °C. It can be seen that at pH = 11, PMS was almost completely consumed until 180 min. Another study reported that an increase in pH could result in PMS decay [72]. In a study on the base-activated PMS process, Yang et al. [73] reported that excess NaOH inhibited the degradation of methylene blue. Here, lower BTA degradation was attributed to the PMS self-decomposition.

Moreover, the presence of Cl^- significantly hampered the BTA degradation under basic conditions. The BTA removal efficiency decreased from 70% (without Cl^- and pH 11) to 58%. The decomposition of PMS and the dissociation of HOCl under pH 11 could explain the significant hindering of BTA removal. HOCl is a weak acid ($pK_a = 7.49$). When the pH rose to 11, more OCl^- with weak oxidation ability (E_0 = 0.94 V) was produced. Then a series of chain reactions generate other chlorine species leading to a lower BTA removal efficiency [74].

3.3. Quenching experiment

To distinguish the predominant species in BTA degradation in PDS and PMS systems, 50 mM EtOH and TBA were selected as both $SO_4^{\bullet-}$ and $HO^{\bullet}$ radicals scavengers and $HO^{\bullet}$ radical scavengers, respectively. Anipsitakis and Dionisiou [75] indicated that the reaction rate of TBA with $SO_4^{\bullet-}$ was 4×10^5 to 9.1×10^5 M^{-1} s^{-1}, which was much lower than the rate with $HO^{\bullet}$ (3.8×10^8 to 7.6×10^8 M^{-1} s^{-1}). Besides, it was reported that the reaction of α hydrogen-containing alcohols (e.g., EtOH) with $HO^{\bullet}$ occurs with rates around 1.2×10^9 to 2.8×10^9 M^{-1} s^{-1}. In contrast, the reaction rate of EtOH with $SO_4^{\bullet-}$ is 1.6×10^7 to 7.7×10^7 M^{-1} s^{-1} [75].

Fig. 3 indicates that the addition of TBA and EtOH showed an inhibition effect on the BTA degradation and removal rate in both PDS and PMS experiments. The k_{obs} (PDS) decreased from 0.07 to 0.02 min^{-1} when the TBA was added, and k_{obs} (PDS) fell to 0.009 min^{-1} when EtOH was added (Table 1). As for PMS, the k_{obs} (PMS) decreased from 0.03 to 0.013 min^{-1} when the TBA was added, and k_{obs} (PDS) fell to 0.008 min^{-1} when EtOH was added. Based on the calculation, the D% (PDS) was 87% in presence of EtOH, which represented the contribution of

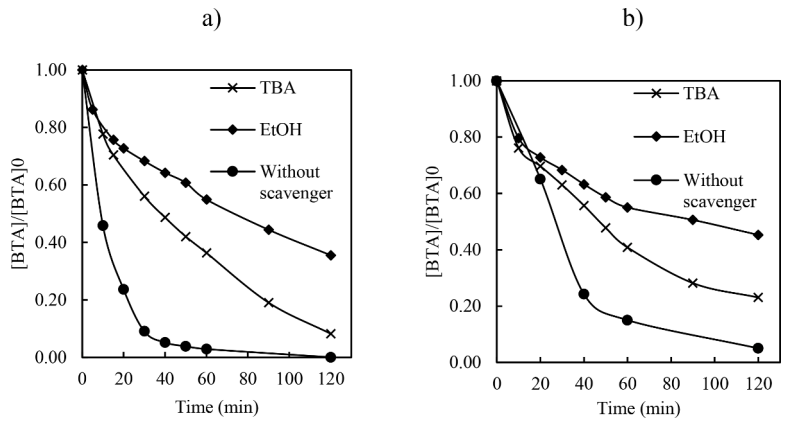

Fig. 3. BTA degradation by (a) PDS and (b) PMS in the presence of radical scavengers (TBA and EtOH) during 120 min reaction. Experimental conditions: $T = 70$ °C, $[BTA]_0 = 0.42$ mM, TBA=50 mM, EtOH=50 mM, $V = 100$ mL; all experiments were buffered by 15 mM phosphate, and sodium hydroxide was added dropwise to maintain the pH of around 6.9–7.4.

Table 1
Influence of scavengers on BTA degradation rate; Experimental conditions: $T = 70$ °C, $[BTA]_0 = 0.42$ mM, [TBA] = [*Et*OH] = [L-*Histidine*] = [sodium azide] = 50 mM, $V = 100$ mL, all experiments were buffered by 15 mM phosphate; sodium hydroxide was added dropwise to maintain the pH around 6.9–7.4.

	k_{obs} (min^{-1})	k_{obs} (D%) with TBA	k_{obs} (D%) with EtOH	k_{obs} (D%) with L-Histidine	k_{obs} (D%) with sodium azide	dominant oxidizing species
PDS	0.07	0.02 (71%)	0.009 (87%)	~0 (99%)	~0 (99%)	$HO^{\bullet}$ /$SO_4^{\bullet-}$
PDS/1000 mg/L Cl^-	0.05	–	–	~0 (99%)	~0 (99%)	
PMS	0.03	0.013 (57%)	0.008 (73%)	~0 (99%)	~0 (99%)	$HO^{\bullet}$ /$SO_4^{\bullet-}$
PMS/1000 mg/L Cl^-	0.3	–	–	~0 (99%)	~0 (99%)	

$SO_4^{\bullet-}$ and $HO^{\bullet}$ to BTA degradation. The D% (PDS) was 71% in presence of TBA, which meant the role of $SO_4^{\bullet-}$ to BTA degradation. As for PMS, The D% (PMS) was 73% and 57% in presence of EtOH and TBA, respectively. The results show that both $HO^{\bullet}$ and $SO_4^{\bullet-}$ were the dominant oxidizing species of BTA degradation in both PDS and PMS experiments.

These results were a little bit different from other studies about PDS. Norman et al. [76] reported no $^{\bullet}OH$ domination when the pH was < 8 in the PDS system. Ji et al. [77] found that 30 mM TBA slightly inhibited ATZ degradation by PDS; $SO_4^{\bullet-}$ was the dominant radical species when pH was 7. Both $HO^{\bullet}$ and $SO_4^{\bullet-}$ contributed to the degradation of organic pollutants when the pH was 9 [78]. The possible explanation of the high contribution of $HO^{\bullet}$ to BTA degradation in our study could be the extra NaOH which was added to maintain the neutral pH because $SO_4^{\bullet-}$ reacted with OH^-, producing $HO^{\bullet}$. To further investigate the domination of ROS, L-histidine and sodium azide were added as $^1O_2$ scavengers. In this way, L-histidine substantially suppressed the oxidative degradation of BTA in as much as no degradation efficiency was observed in both PDS and PMS-based processes, either in the presence or absence of chloride. In PMS-based processes, $^1O_2$ can be produced by PMS self-decomposition. Nonetheless, due to the rapid depletion of PMS as exposed to L-histidine, domination of $^1O_2$ cannot be confirmed in the studied PMS-based processes. This finding was similar to the results obtained in the study conducted by Gao et al. [79], in which L-histidine suppressed the bisphenol A degradation in the NCN-900/PMS process. The following equations show the possible generation of $^1O_2$ in PMS-based processes Eqs. (7)-(8) [80].

$$HSO_5^- \rightarrow SO_5^{\bullet-} + H^+ + e^- \quad (7)$$

$$2SO_5^{\bullet-} + H_2O \rightarrow 2HSO_4^- + 1.5\ ^1O_2 \quad (8)$$

Likewise, the addition of sodium azide remarkably inhibited the BTA degradation efficiency. However, due to their direct reaction with PMS, L-histidine and sodium azide are not supposedly indicative for determining the dominant ROS in PMS-based processes. Also, in the PDS-based process, L-histidine and sodium azide inhibited the BTA degradation substantially, representing the possible domination of $^1O_2$. One hypothesis is that the C=O group can be the intermediate precursor for forming $^1O_2$ [80]. This structure was also identified amongst the BTA degradation intermediates.

3.4. Mineralization, degradation products, and their evolution pathways

According to the results obtained in LC-MS/MS analysis in both positive and negative modes, 42 TPs were detected (Table S2). BTA degradation pathways were proposed in PDS and PMS-based processes (Fig. 4). This survey was carried out in presence and absence of Cl^- to track the TPs and seek possible changes in the BTA degradation pathway. In absence of chloride, four different pathways were hypothesized, as in Fig. 4a. The major degradation mechanisms for BTA were hydroxylation, benzene ring-opening, bond cleavage, and carboxylic acid formation. Surprisingly, in many of the identified TPs, the triazole ring remained stable due to its higher persistence in degradation. A study by Jorfi et al. [22] stated a different finding. They hypothesized that BTA degradation was initiated by triazole ring-opening or destruction of the double-bonded nitrogen in the triazole ring. In another study on the degradation of 4- and 5-methyl-1H-benzotriazole, the triazole ring remained intact [81]. Regarding the identified TPs in Table S3, it can be seen that nitric acid (TP27) was identified in PDS and PMS-based processes, both in the presence and absence of chloride. Of note, in absence of chloride, nitric acid was merely identified at reaction times of as long as 120 and 180 min. While in presence of chloride, it was observed that nitric acid was also detected at much shorter reaction times; at 10, 30, and 60 min (Table S3). Considering the identified TPs, triazole ring-opening occurred when chloride was there within the solution, and the triazole ring was the only nitrogen source in the studied matrix. In other words, detection of nitric acid indicated triazole ring-opening; the rate of this ring-opening reaction appears to be boosted in the presence of chloride, especially in PMS/Cl^- process. It has been found that presence of chloride at high concentrations (> 100 mM) can enhance the degradation rate of nitrogen-containing rings and bonds as they occur in azo dyes [37,82]. Occurrence of polymerization

(a)

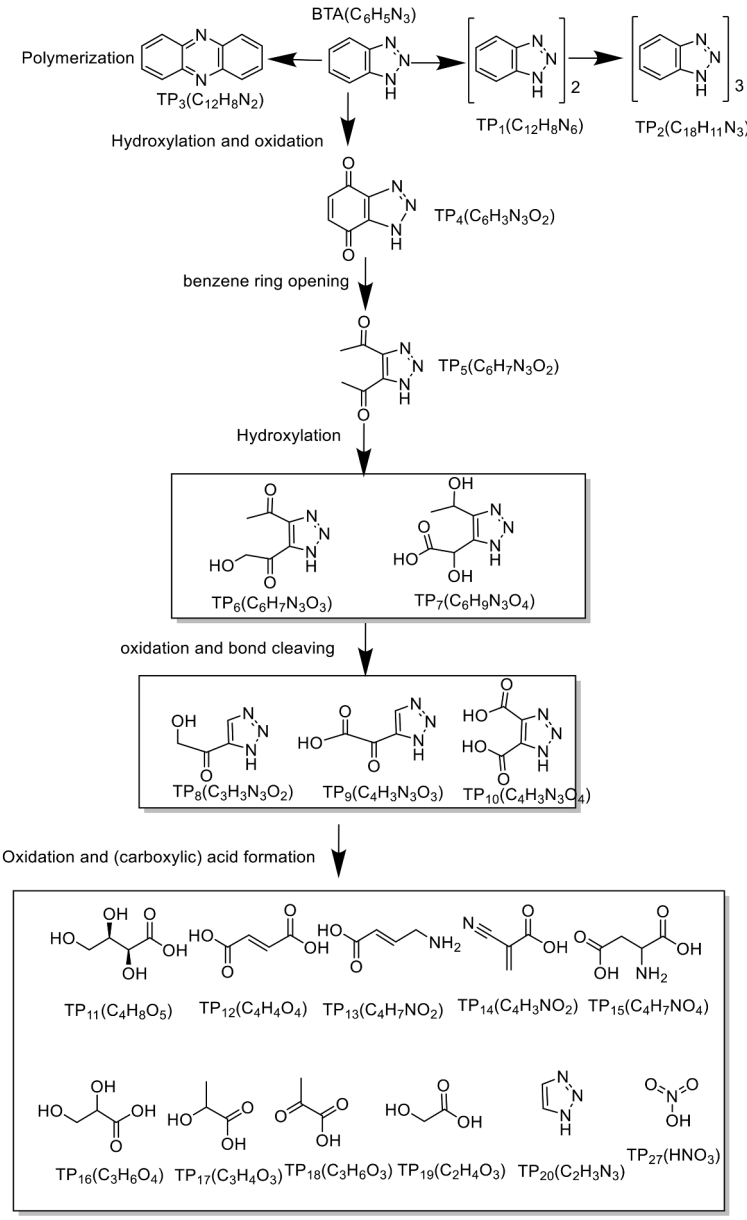

Fig. 4(. a). Proposed BTA degradation pathways during heat-activated PDS/PMS oxidation in absence of Cl^-, Experimental conditions: $T = 70$ °C, $[BTA]_0 = 0.42$ mM, $[PDS]_0$ or $[PMS]_0 = 15$ mM, $[Cl^-] = 0$ or 1000 mg/L, $V = 100$ mL, sodium hydroxide was added dropwise to maintain the pH around 6.9–7.4. (b). Proposed BTA degradation pathways during heat-activated PDS/PMS oxidation in presence of Cl^-, Experimental conditions: $T = 70$ °C, $[BTA]_0 = 0.42$ mM, $[PDS]_0$ or $[PMS]_0 = 15$ mM, $[Cl^-] = 0$ or 1000 mg/L, $V = 100$ mL, sodium hydroxide was added dropwise to maintain the pH around 6.9–7.4.

was detected by identifying TP1 and TP2 representing $C_{12}H_8N_6$ and $C_{18}H_{11}N_9$ with *m/z* of Ca. 236 and 353, respectively. Regarding Table S3, the TPs mentioned earlier were identified from the beginning of the degradation reactions in 10 min remaining in the solution until over 120 min. Anyway, polymerization is a common mechanism at the beginning of the degradation pathway [19]. BTA also underwent hydroxylation followed by benzene ring-opening and bond cleavage as reflected by the identification of TP4-TP10, especially in absence of chloride. These intermediates were shown up in 10-180 min reaction time as in Table S3. Afterward, the intermediates were further oxidized into carboxylic acids. It is worth noting that the solo triazole ring was merely detectable in 180 min within both PDS and PMS-based processes in the absence of Cl^-.

In the case of chloride-laden samples, 28 TPs were detected; many of them were chlorinated. As in Fig. 4b, BTA degradation was hypothesized to follow a multilateral pathway, including the previously mentioned mechanisms as well as chlorination of BTA, TPs, and carboxylic acids. In PMS/Cl^-, more chlorinated TPs were detected in comparison with PDS/Cl^-. This finding was in agreement with the results obtained in the mineralization study. As Table 2 indicated, PDS-based processes brought about higher mineralization. Using PDS, 90% and 76% TOC removals were obtained in the absence and presence of chloride, respectively. Based on LC-MS/MS analysis results, many TPs, particularly TP28-TP35, demonstrated the addition of a chlorine atom to the aromatic structures, making the compound more persistent to oxidative degradation. On the contrary, chloride exhibited a positive effect on TOC removal in a PMS-

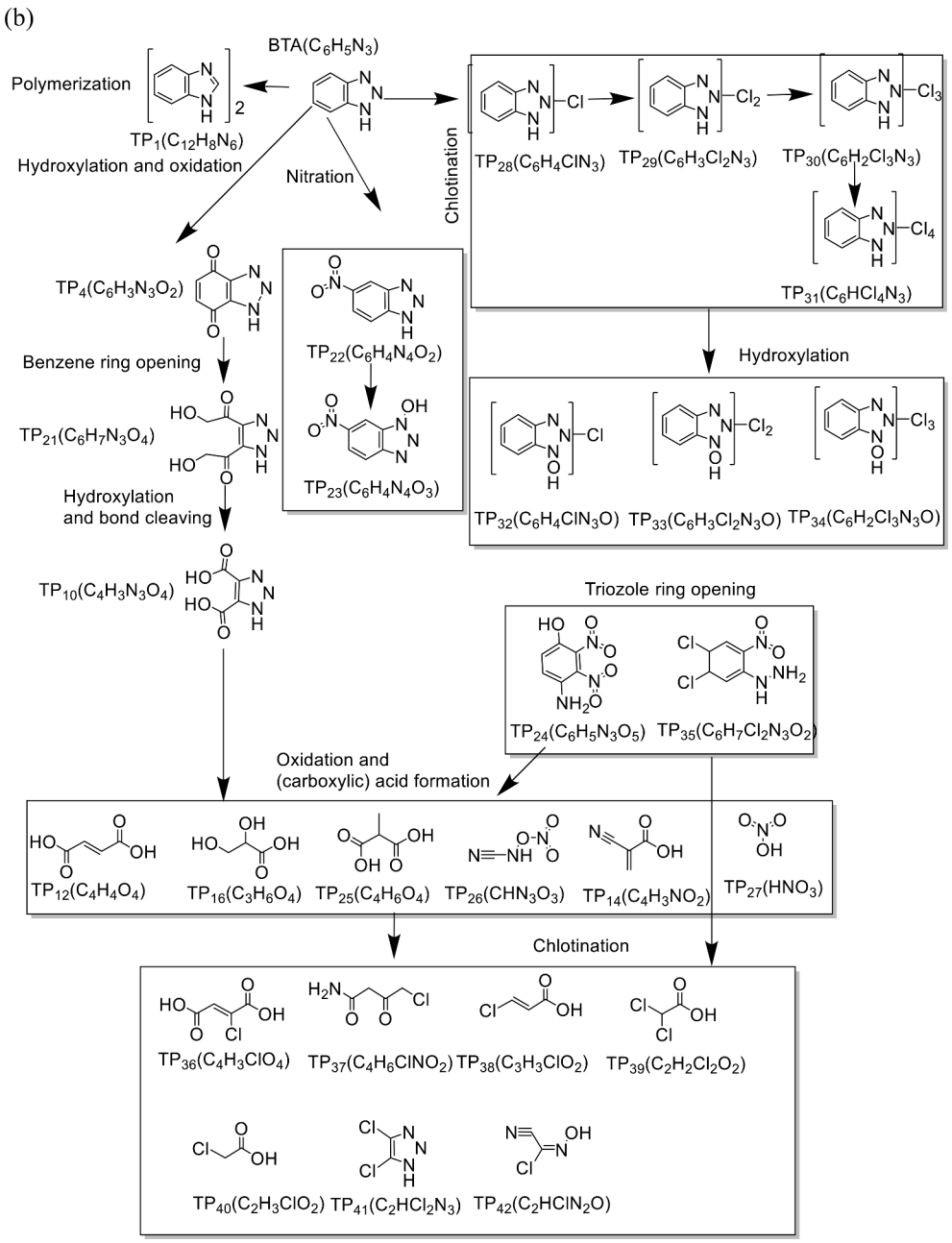

Fig. 4(. (*continued*).

Table 2
BTA mineralization in presence and absence of Cl^-after 180 min reaction; Experimental conditions: $T = 70$ °C, $[BTA]_0 = 0.42$ mM, $[PDS]_0 = [PMS]_0 = 15$ mM, $V = 100$ mL, all experiments were buffered by 15 mM phosphate, and sodium hydroxide was added dropwise to maintain the pH around 6.9–7.4.

	Cl^- (mg/L)	Mineralization (%)
PDS	0	90
	1000	76
PMS	0	14
	1000	43

based process, similar to the results obtained and discussed for BTA removal. However, the application of PMS led to far less mineralization (%) as compared to that of PDS (Table 2). As depicted in Fig 4b, many chlorinated TPs such as TP22, TP23, TP29, TP31, TP32, TP33, and TP34 were formed in the PMS-based process and were mostly persistent until 180 min reaction time. Although the BTA removal rate was significantly high in PMS/Cl^- than in PMS (as discussed in the kinetic study), it was initially transformed into chlorinated BTA species through the third and fourth pathways (Fig. 4b) with no significant mineralization. Nevertheless, the second pathway mainly consisted of hydroxylation, bond cleavage, benzene, and triazole ring-opening leading to some degrees of mineralization. To sum up, in presence of chloride, heat/PDS revealed better results than heat/PMS from the aspect of TPs formation and mineralization.

3.5. AOX formation

PDS is a symmetrical peroxide that is almost inert to anionic nucleophiles like chloride. However, as an asymmetrical oxidant, PMS reactivity in nucleophilic addition, e.g., in reaction with chloride as a common anion of water, makes the reactions complex. Although Cl^- can act as a $SO_4^{\bullet-}$ scavenger, it can concurrently induce another degradation

pathway through direct reaction with PMS leading to the formation of free chlorine species (Environ. Sci. Technol. 2021, 55, 5382−5392). LC-MS/MS analysis shows that chlorinated transformation products (TPs) are formed and accumulated during BTA oxidation in presence of Cl^-. After the treatment, the AOX concentration was measured to assess the total chlorinated TPs (Table 3). The AOX concentration of both PDS and PMS experiments increased gradually with the increase of Cl^- concentration. Cl^- concentration from 100 to 10,000 mg/L increased the AOX concentration from 2.5 to 9.1 mg/L in PDS and from 6.5 to 19.5 mg/L in the PMS system. Meanwhile, at the same concentration of Cl^-, the PMS system formed more AOX than PDS. Applying 100 and 10,000 mg/L Cl^- in the PMS system, the AOX level was almost 2 to 3 times that in the PDS system. More free chlorine was formed due to PMS and Cl^- reaction. The oxygen atom transfer from PMS to halides is an endothermic reaction; thus, the temperature elevation probably favors the generation of HOCl that occurs exclusively with PMS [28]. It is hypothesized that the generated free chlorine could chlorinate the BTA directly to produce AOX.

The AOX level was proportional to the Cl^- level in the Acid Orange 7 degradation in UV/TiO_2 [83]. AOX is harmful to human health and the ecosystem, and increasing AOX means increasing toxicity. The industrial wastewater treatment effluent's AOX should be lower than 0.5 mg/L [84]. The AOX level of our experiments was much higher than 0.5 mg/L crying out for minimization. Applying PDS to treat chloride-containing matrix, chlorine radicals dominantly attack the aromatic ring or double bond, leading to AOX formation. While in the case of PMS-based processes, both chlorine radical and free chlorine predominate, inducing aromatic ring or double bond cleavage and direct chlorination, respectively.

Fang et al. [85] evaluated the effect of chloride on degradation kinetic using AOPs, focusing on AOX evolution. The studied Co/PMS process was more reactive under acidic conditions leading to high levels of AOX. They stated that high chloride levels resulted in AOX accumulation within the Co/PMS process [85]. Thus, it was found that initial pH highly affected AOX formation during PMS-based AOPs. It was concluded that PMS-based advanced oxidation processes are not recommended to treat highly saline wastewater, regardless of their efficiency in high rate degradation of target organic pollutants [85].

3.6. Free chlorine and chlorates formation

In the present study, the formation of free chlorine and ClO_3^- after 180 min reaction in the PDS and PMS process in presence of Cl^- was investigated and shown in Table 3. Only a small concentration of free chlorine and no ClO_3^- was observed in the PDS process at any concentration of Cl^-. PMS produced certain amounts of free chlorine and ClO_3^- at any concentration of Cl^-. Additionally, with the increase of Cl^- concentration, the amount of free chlorine and ClO_3^- increased. The formation of ClO_3^- was raised by a factor of 3.5 when the concentration of Cl^- was 100 mg/L and 10,000 mg/L. Free chlorine is the precursor for ClO_3^- formation. In the PDS system, $SO_4^{\bullet-}$ rather than PDS, reacts with Cl^- generating free chlorine, while in the PMS-based process, apart from the radical pathway, PMS directly reacts with chloride leading to the generation of free chlorine. Thus, 98 mg/L free chlorine and 17 mg/L ClO_3^- were formed in the 1000 mg/L Cl^-/ PMS process at 25 °C (Table 3). At 25 °C, radical formation is limited, and ClOx formation is mainly mediated by direct PMS and Cl^- reaction. Hou et al. [45] comprehensively investigated chlorate formation in the co-exposure of SO_4^{2-}, Cl^- and organics in PDS and PMS-based processes. They also reported a higher generation of ClO_3^- in the PMS-based process than the PDS process. It was mentioned that the application of sulfate radical-based AOPs needs more attention in acidic pH.

Table 3
AOX, free chlorine and chlorate formation, as well as toxicity in terms of% luminescent inhabitation during BTA degradation at various Cl^- concentrations after 180 min: Experimental conditions: $T = 70$ °C, $[BTA]_0 = 0.42$ mM, $[PDS]_0$ or $[PMS]_0 = 15$ mM, $V = 100$ mL, sodium hydroxide was added dropwise to maintain the pH around 6.9–7.4.

	Cl^-(mg/L)	AOX (mg/L as Cl_2)	Free chlorine (mg/L Cl_2)	ClO_3^- (mg/L)	Increase of inhibition (%)
PDS	100	2.5	1.4	ND	9
	1000	7.5	2.5	ND	14
	1000 (25°C)	–	–	ND	–
	10,000	9.1	2.4	ND	36
PMS	100	6.5	4.6	9.6	17
	1000	9.4	65	14.0	21
	1000 (25°C)	–	98	16.7	–
	10,000	19.5	223	32.3	42

3.7. Toxicity of degradation products

Luminescent bacteria were used to analyze the toxicity in both PDS and PMS systems. The raising of luminescence inhibition represents the increase of toxicity in samples. Table 3 summarizes the toxicity of each sample. Bacteria are sensitive to environmental changes, so the micro-toxicity experiments are not quantitative. After the reaction in 100 mg/L Cl^-, the luminescence inhibition was increased by 9% and 17% in PDS and PMS experiments, respectively. The luminescence inhibition was increased by 14% and 21%, at 1000 mg/L Cl^-, and to 35.67% (PDS) and 42.00% (PMS), at 10,000 mg/L Cl^-. Overall, the higher the Cl^- concentration, the higher value of inhibition was obtained. These results also reflect two effects: i) the PMS system produced more AOX than the PDS system at any Cl^- concentration, and ii) the accumulation of AOX increased the toxicity [86].

4. Conclusions

This study shows that heat-activated PDS/PMS is capable of degrading BTA. PDS outcompeted the PMS process in the absence of Cl^-; however, PMS outcompeted the PDS process in presence of Cl^-. Both $HO^{\bullet}$ and $SO_4^{\bullet-}$ radicals contributed to BTA degradation in PDS and PMS systems. BTA degradation in PDS was barely affected by pH. In contrast, pH 7 was the best condition for PMS performance. Although a higher degradation rate at pH 11 was initially seen in PMS, after 20 min, less BTA degradation was observed since the PMS was easy to decompose under basic conditions. In the PDS experiment, a low concentration (100 mg/L) of Cl^- slightly reduced the BTA degradation rate, but higher concentrations (1000 mg/L or 10,000 mg/L) inhibited the reaction significantly because of radical scavenging. In PMS, increasing Cl^- concentration significantly increased the reaction rate at the optimum condition at a Cl^- concentration of 1000 mg/L due to active chlorine formation. Generally, in degradation processes like AOPs especially in presence of matrix constituents like Cl^-, as in real samples and large-scale applications, transformation products e.g. AOX and ClO_x should be monitored and must be taken into account for the selection and optimization of the treatment processes. In this study, measurement of non-radical chlorinated species (free chlorine) was carried out, while radical chlorine species' detection is proposed for further investigation. At any concentration of Cl^-, both PDS and PMS produced a significant amount of AOX. PMS produced more AOX than PDS. Transformation products (TPs) analysis showed that degradation pathways were significantly altered in presence of Cl^-. Polymerization, hydroxylation, benzene ring-opening, and carboxylic acid formation were the common degradation steps with and without Cl^-. However, the Triazole ring was broken quickly in presence of Cl^-, whereas it was more stable in the absence of Cl^-. In addition, chlorination reaction dominated, producing several chlorinated TPs, including chlorinated BTA and chlorinated carboxylic acids. The micro-toxicity test indicated that the toxicity increased in the treated samples in presence of Cl^- due to the formation of chlorinated TPs. These by-products were more toxic than the parent

compound in both PDS and PMS. No chlorate was formed in PDS at any Cl^- concentration, but, ClO_3^- was found in the PMS system. Besides, higher luminescence inhibition was observed in PMS system in presence of chloride with more AOX formation. Further investigations on possible inhibitory effects related to the residual oxidants, e.g., PDS and PMS, can be considered in future studies. These findings may help better understand the influence of Cl^- in the BTA degradation rate and pathway in PDS and PMS base oxidation. To avoid AOX formation, as little as possible Cl^- is recommended.

CRediT authorship contribution statement

Pradip Saha: Conceptualization, Methodology, Investigation, Formal analysis, Writing – original draft, Writing – review & editing. **Chenyu Zhou:** Investigation, Formal analysis, Writing – original draft. **Mahsa Moradi:** Conceptualization, Writing – review & editing. **Huub H.M. Rijnaarts:** Supervision, Writing – review & editing, Funding acquisition. **Harry Bruning:** Conceptualization, Supervision, Writing – original draft, Writing – review & editing.

Declaration of Competing Interest

The authors declare that they have no known competing financial interests or personal relationships that could have appeared to influence the work reported in this paper.

Data availability

Data will be made available on request.

Acknowledgments

This research is financed by the Netherlands Organization for Scientific Research (NWO), which is partly funded by the Ministry of Economic Affairs and Climate Policy and co-financed by the Netherlands Ministry of Infrastructure and Water Management and partners of the Dutch Water Nexus consortium (project number 14301).

Supplementary materials

Supplementary material associated with this article can be found, in the online version, at doi:10.1016/j.ceja.2023.100472.

References

[1] NORMAN, NORMAN list of emerging substances, 2016. https://www.norman-network.net/?q=node/81. (Accessed 07.07 2020).
[2] C.E. Smit, S. Wuijts, Specific Pollutants and Drinking Water Relevant Substances in the Context of the Water Framework Directive: Selection of Potentially Relevant Substances For the Netherlands, National Institute for Public Health and the Environment RIVM, The Netherlands, 2012.
[3] J.E. Lee, M.K. Kim, J.Y. Lee, Y.M. Lee, K.D. Zoh, Degradation kinetics and pathway of 1H-benzotriazole during UV/chlorination process, Chem. Eng. J. 359 (2019) 1502–1508, https://doi.org/10.1016/j.cej.2018.11.026.
[4] J.L. Wu, Q. Xiong, J.L. Liang, Q. He, D.X. Yang, R.Y. Deng, Y. Chen, Degradation of benzotriazole by DBD plasma and peroxymonosulfate: mechanism, degradation pathway and potential toxicity, Chem. Eng. J. 384 (2020), https://doi.org/10.1016/j.cej.2019.123300.
[5] Y. Ding, C. Yang, L. Zhu, J. Zhang, Photoelectrochemical activity of liquid phase deposited TiO2 film for degradation of benzotriazole, J. Hazard. Mater. 175 (1–3) (2010) 96–103, https://doi.org/10.1016/j.jhazmat.2009.09.037.
[6] J. Hollingsworth, R. Sierra-Alvarez, M. Zhou, K.L. Ogden, J.A. Field, Anaerobic biodegradability and methanogenic toxicity of key constituents in copper chemical mechanical planarization effluents of the semiconductor industry, Chemosphere 59 (9) (2005) 1219–1228, https://doi.org/10.1016/j.chemosphere.2004.11.067.
[7] Y.S. Liu, G.G. Ying, A. Shareef, R.S. Kookana, Biodegradation of three selected benzotriazoles under aerobic and anaerobic conditions, Water Res. 45 (16) (2011) 5005–5014, https://doi.org/10.1016/j.watres.2011.07.001.
[8] A. Seeland, M. Oetken, A. Kiss, E. Fries, J. Oehlmann, Acute and chronic toxicity of benzotriazoles to aquatic organisms, Environ. Sci. Pollut. Res. Int. 19 (5) (2012) 1781–1790, https://doi.org/10.1007/s11356-011-0705-z.
[9] C.K. Groot, W.B. van den Broek, J. Loewenberg, N. Koeman-Stein, M. Heidekamp, W. de Schepper, Mild desalination of various raw water streams, Water Sci. Technol. 72 (3) (2015) 371–376, https://doi.org/10.2166/wst.2015.228.
[10] N.E. Koeman-Stein, R.J.M. Creusen, M. Zijlstra, C.K. Groot, W.B.P. van den Broek, Membrane distillation of industrial cooling tower blowdown water, Water Resour. Ind. 14 (2016) 11–17, https://doi.org/10.1016/j.wri.2016.03.002.
[11] S. de Mendonça Ochs, T.M. Souza, R.d.L. Sobrinho, R.B. de Oliveira, M. C. Bernardes, A.D.P. Netto, Simultaneous evaluation of benzotriazoles, benzothiazoles and benzenesulfonamides in water samples from the impacted urban Jacarepaguá Lagoon System (Rio de Janeiro, Brazil) by liquid chromatography coupled to electrospray tandem mass spectrometry, Sci. Total Environ. 858 (2023), 160033, https://doi.org/10.1016/j.scitotenv.2022.160033.
[12] M.G. Cantwell, J.C. Sullivan, D.R. Katz, R.M. Burgess, J. Bradford Hubeny, J. King, Source determination of benzotriazoles in sediment cores from two urban estuaries on the Atlantic Coast of the United States, Mar. Pollut. Bull. 101 (1) (2015) 208–218, https://doi.org/10.1016/j.marpolbul.2015.10.075.
[13] M.G. Cantwell, J.C. Sullivan, R.M. Burgess, Benzotriazoles, persistent organic pollutants (POPs): analytical techniques, Environ. Fate Biol. Effects (2015) 513–545, https://doi.org/10.1016/b978-0-444-63299-9.00016-8.
[14] T. Yang, J. Mai, S. Wu, C. Liu, L. Tang, Z. Mo, M. Zhang, L. Guo, M. Liu, J. Ma, UV/chlorine process for degradation of benzothiazole and benzotriazole in water: efficiency, mechanism and toxicity evaluation, Sci. Total Environ. 760 (2021), 144304, https://doi.org/10.1016/j.scitotenv.2020.144304.
[15] Y. Zhang, H. Ji, W. Liu, Z. Wang, Z. Song, Y. Wang, C. Liu, B. Xu, F. Qi, Synchronous degradation of aqueous benzotriazole and bromate reduction in catalytic ozonation: effect of matrix factor, degradation mechanism and application strategy in water treatment, Sci. Total Environ. 727 (2020), 138696, https://doi.org/10.1016/j.scitotenv.2020.138696.
[16] M. Minella, E. De Laurentiis, F. Pellegrino, M. Prozzi, F. Dal Bello, V. Maurino, C. Minero, Photocatalytic transformations of 1H-Benzotriazole and Benzotriazole derivates, Nanomaterials (Basel) 10 (9) (2020), https://doi.org/10.3390/nano10091835.
[17] Y. Liu, W.L. Guo, H.S. Guo, X.H. Ren, Q. Xu, Cu (II)-doped V2O5 mediated persulfate activation for heterogeneous catalytic degradation of benzotriazole in aqueous solution, Sep. Purif. Technol. 230 (2020), https://doi.org/10.1016/j.seppur.2019.115848.
[18] X.R. Li, D.M. Zhang, Z.H. Liu, C. Lyu, S. Niu, Z.J. Dong, C. Lyu, Enhanced catalytic oxidation of benzotriazole via peroxymonosulfate activated by CoFe2O4 supported onto nitrogen-doped three-dimensional graphene aerogels, Chem. Eng. J. 400 (2020), https://doi.org/10.1016/j.cej.2020.125897.
[19] F. Ghanbari, M. Khatebasreh, M. Mahdavianpour, K.A. Lin, Oxidative removal of benzotriazole using peroxymonosulfate/ozone/ultrasound: synergy, optimization, degradation intermediates and utilizing for real wastewater, Chemosphere 244 (2020), 125326, https://doi.org/10.1016/j.chemosphere.2019.125326.
[20] J. Ye, H. Hu, Y. Chen, Y. Chen, H. Ou, Degradation of 1H-benzotriazole using vacuum ultraviolet: a prospective treatment method for micro-pollutants, Water Sci. Technol. 80 (4) (2019) 773–783, https://doi.org/10.2166/wst.2019.320.
[21] J. Ma, Y. Ding, L. Chi, X. Yang, Y. Zhong, Z. Wang, Q. Shi, Degradation of benzotriazole by sulfate radical-based advanced oxidation process, Environ. Technol. (2019) 1–10, https://doi.org/10.1080/09593330.2019.1625959.
[22] S. Jorfi, B. Kakavandi, H.R. Motlagh, M. Ahmadi, N. Jaafarzadeh, A novel combination of oxidative degradation for benzotriazole removal using TiO2 loaded on FeIIFe2IIIO4@C as an efficient activator of peroxymonosulfate, Appl. Catal. B Environ. 219 (2017) 216–230, https://doi.org/10.1016/j.apcatb.2017.07.035.
[23] E. Felis, A. Sochacki, S. Magiera, Degradation of benzotriazole and benzothiazole in treatment wetlands and by artificial sunlight, Water Res. 104 (2016) 441–448, https://doi.org/10.1016/j.watres.2016.08.037.
[24] E. Borowska, E. Felis, J. Kalka, Oxidation of benzotriazole and benzothiazole in photochemical processes: kinetics and formation of transformation products, Chem. Eng. J. 304 (2016) 852–863, https://doi.org/10.1016/j.cej.2016.06.123.
[25] F. Ghanbari, M. Moradi, Application of peroxymonosulfate and its activation methods for degradation of environmental organic pollutants: review, Chem. Eng. J. 310 (2017) 41–62, https://doi.org/10.1016/j.cej.2016.10.064.
[26] S. Giannakis, K.Y.A. Lin, F. Ghanbari, A review of the recent advances on the treatment of industrial wastewaters by Sulfate Radical-based Advanced Oxidation Processes (SR-AOPs), Chem. Eng. J. 406 (2021), https://doi.org/10.1016/j.cej.2020.127083.
[27] W. Peng, Y. Dong, Y. Fu, L. Wang, Q. Li, Y. Liu, Q. Fan, Z. Wang, Non-radical reactions in persulfate-based homogeneous degradation processes: a review, Chem. Eng. J. 421 (2021), https://doi.org/10.1016/j.cej.2020.127818.
[28] Y.-Y. Ahn, J. Choi, M. Kim, M.S. Kim, D. Lee, W.H. Bang, E.-T. Yun, H. Lee, J.-H. Lee, C. Lee, S.K. Maeng, S. Hong, J. Lee, Chloride-mediated enhancement in heat-induced activation of peroxymonosulfate: new reaction pathways for oxidizing radical production, Environ. Sci. Technol. 55 (8) (2021) 5382–5392, https://doi.org/10.1021/acs.est.0c07964.
[29] R.Y. Xiao, Z.H. Luo, Z.S. Wei, S. Luo, R. Spinney, W.C. Yang, D.D. Dionysiou, Activation of peroxymonosulfate/persulfate by nanomaterials for sulfate radical-based advanced oxidation technologies, Curr. Opin. Chem. Eng. 19 (2018) 51–58, https://doi.org/10.1016/j.coche.2017.12.005.
[30] J.L. Wang, S.Z. Wang, Activation of persulfate (PS) and peroxymonosulfate (PMS) and application for the degradation of emerging contaminants, Chem. Eng. J. 334 (2018) 1502–1517, https://doi.org/10.1016/j.cej.2017.11.059.
[31] H.D. Xu, N. Jiang, D. Wang, L.H. Wang, Y.F. Song, Z.Q. Chen, J. Ma, T. Zhang, Improving PMS oxidation of organic pollutants by single cobalt atom catalyst through hybrid radical and non-radical pathways, Appl. Catal. B-Environ. 263 (2020), https://doi.org/10.1016/j.apcatb.2019.118350.

[32] W. Zhang, S. Zhou, J. Sun, X. Meng, J. Luo, D. Zhou, J. Crittenden, Impact of chloride ions on UV/H2O2 and UV/persulfate advanced oxidation processes, Environ. Sci. Technol. 52 (13) (2018) 7380–7389, https://doi.org/10.1021/acs.est.8b01662.
[33] P. Caregnato, J.A. Rosso, J.M. Soler, A. Arques, D.O. Martire, M.C. Gonzalez, Chloride anion effect on the advanced oxidation processes of methidathion and dimethoate: role of Cl2(.-) radical, Water Res. 47 (1) (2013) 351–362, https://doi.org/10.1016/j.watres.2012.10.018.
[34] Y.X. Wu, Y. Yang, Y.Z. Liu, L.Q. Zhang, L. Feng, Modelling study on the effects of chloride on the degradation of bezafibrate and carbamazepine in sulfate radical-based advanced oxidation processes: conversion of reactive radicals, Chem. Eng. J. 358 (2019) 1332–1341, https://doi.org/10.1016/j.cej.2018.10.125.
[35] Y. Lei, C.-.S. Chen, J. Ai, H. Lin, Y.-.H. Huang, H. Zhang, Selective decolorization of cationic dyes by peroxymonosulfate: non-radical mechanism and effect of chloride, RSC Adv. 6 (2) (2016) 866–871, https://doi.org/10.1039/C5RA19718J.
[36] R. Yuan, S.N. Ramjaun, Z. Wang, J. Liu, Effects of chloride ion on degradation of Acid Orange 7 by sulfate radical-based advanced oxidation process: implications for formation of chlorinated aromatic compounds, J. Hazard. Mater. 196 (2011) 173–179, https://doi.org/10.1016/j.jhazmat.2011.09.007.
[37] Z. Wang, R. Yuan, Y. Guo, L. Xu, J. Liu, Effects of chloride ions on bleaching of azo dyes by Co2+/oxone reagent: kinetic analysis, J. Hazard. Mater. 190 (1–3) (2011) 1083–1087, https://doi.org/10.1016/j.jhazmat.2011.04.016.
[38] P. Wang, S. Yang, L. Shan, R. Niu, X. Shao, Involvements of chloride ion in decolorization of Acid Orange 7 by activated peroxydisulfate or peroxymonosulfate oxidation, J. Environ. Sci. (China) 23 (11) (2011) 1799–1807, https://doi.org/10.1016/s1001-0742(10)60620-1.
[39] Z. Wang, M. Feng, C. Fang, Y. Huang, L. Ai, F. Yang, Y. Xue, W. Liu, J. Liu, Both degradation and AOX accumulation are significantly enhanced in UV/peroxymonosulfate/4-chlorophenol/Cl− system: two sides of the same coin? RSC Adv. 7 (20) (2017) 12318–12321, https://doi.org/10.1039/c7ra01294b.
[40] C.L. Fang, X.Y. Lou, Y. Huang, M. Feng, Z.H. Wang, J.S. Liu, Monochlorophenols degradation by UV/persulfate is immune to the presence of chloride: illusion or reality? Chem. Eng. J. 323 (2017) 124–133, https://doi.org/10.1016/j.cej.2017.04.094.
[41] J.S. Ye, P.L. Zhou, Y. Chen, H.S. Ou, J. Liu, C.S. Li, Q.S. Li, Degradation of 1H-benzotriazole using ultraviolet activating persulfate: mechanisms, products and toxicological analysis, Chem. Eng. J. 334 (2018) 1493–1501, https://doi.org/10.1016/j.cej.2017.11.101.
[42] W.-.D. Oh, S.-.K. Lua, Z. Dong, T.-.T. Lim, A novel three-dimensional spherical CuBi 2 O 4 consisting of nanocolumn arrays with persulfate and peroxymonosulfate activation functionalities for 1 H-benzotriazole removal, Nanoscale 7 (17) (2015) 8149–8158.
[43] H.V. Lutze, N. Kerlin, T.C. Schmidt, Sulfate radical-based water treatment in presence of chloride: formation of chlorate, inter-conversion of sulfate radicals into hydroxyl radicals and influence of bicarbonate, Water Res. 72 (2015) 349–360, https://doi.org/10.1016/j.watres.2014.10.006.
[44] Y. Qian, X. Guo, Y. Zhang, Y. Peng, P. Sun, C.H. Huang, J. Niu, X. Zhou, J. C. Crittenden, Perfluorooctanoic Acid Degradation Using UV-Persulfate Process: modeling of the Degradation and Chlorate Formation, Environ. Sci. Technol. 50 (2) (2016) 772–781, https://doi.org/10.1021/acs.est.5b03715.
[45] S. Hou, L. Ling, D.D. Dionysiou, Y. Wang, J. Huang, K. Guo, X. Li, J. Fang, Chlorate formation mechanism in the presence of sulfate radical, chloride, bromide and natural organic matter, Environ. Sci. Technol. 52 (11) (2018) 6317–6325, https://doi.org/10.1021/acs.est.8b00576.
[46] WHO, Chemical hazards in drinking-water: chlorine dioxide, Chlorate Chlorite (2005).
[47] L.B. Peng, D.Y. Deng, F.T. Ye, Efficient oxidation of high levels of soil-sorbed phenanthrene by microwave-activated persulfate: implication for in situ subsurface remediation engineering, J. Soils Sediments 16 (1) (2016) 28–37, https://doi.org/10.1007/s11368-015-1176-5.
[48] I.A. Ike, K.G. Linden, J.D. Orbell, M. Duke, Critical review of the science and sustainability of persulphate advanced oxidation processes, Chem. Eng. J. 338 (2018) 651–669, https://doi.org/10.1016/j.cej.2018.01.034.
[49] I.A. Ike, J.D. Orbell, M. Duke, Activation of Persulfate at Waste Heat Temperatures for Humic Acid Degradation, ACS Sustain. Chem. Eng. 6 (3) (2018) 4345–4353, https://doi.org/10.1021/acssuschemeng.7b04840.
[50] J.L. Wang, S.Z. Wang, Reactive species in advanced oxidation processes: formation, identification and reaction mechanism, Chem. Eng. J. 401 (2020), https://doi.org/10.1016/j.cej.2020.126158.
[51] S.O. Ganiyu, C.A. Martinez-Huitle, M.A. Oturan, Electrochemical advanced oxidation processes for wastewater treatment: advances in formation and detection of reactive species and mechanisms, Curr. Opin. Electrochem. 27 (2021), https://doi.org/10.1016/j.coelec.2020.100678.
[52] S. Gokulakrishnan, A. Mohammed, H. Prakash, Determination of persulphates using N, N-diethyl-p-phenylenediamine as colorimetric reagent: oxidative coloration and degradation of the reagent without bactericidal effect in water, Chem. Eng. J. 286 (2016) 223–231.
[53] Z. Fang, R. Huang, P. Chelme-Ayala, Q. Shi, C. Xu, M. Gamal El-Din, Comparison of UV/Persulfate and UV/H2O2 for the removal of naphthenic acids and acute toxicity towards Vibrio fischeri from petroleum production process water, Sci. Total Environ. 694 (2019), 133686, https://doi.org/10.1016/j.scitotenv.2019.133686.
[54] W.E. Federation, Standard Methods For The Examination Of Water And Wastewater, 21 ed., American Public Health Association (APHA), Washington, DC, USA, 2005.
[55] G.P. Anipsitakis, T.P. Tufano, D.D. Dionysiou, Chemical and microbial decontamination of pool water using activated potassium peroxymonosulfate, Water Res. 42 (12) (2008) 2899–2910, https://doi.org/10.1016/j.watres.2008.03.002.
[56] G.P. Anipsitakis, D.D. Dionysiou, M.A. Gonzalez, Cobalt-mediated activation of peroxymonosulfate and sulfate radical attack on phenolic compounds. implications of chloride ions, Environ. Sci. Technol. 40 (3) (2006) 1000–1007, https://doi.org/10.1021/es050634b.
[57] Y. Deng, C.M. Ezyske, Sulfate radical-advanced oxidation process (SR-AOP) for simultaneous removal of refractory organic contaminants and ammonia in landfill leachate, Water Res. 45 (18) (2011) 6189–6194, https://doi.org/10.1016/j.watres.2011.09.015.
[58] G.V. Buxton, M. Bydder, G.A. Salmon, The reactivity of chlorine atoms in aqueous solution Part II. The equilibrium SO 4-+ Cl-Cl Nsbd+ SO 4 2, Phys. Chem. Chem. Phys. 1 (2) (1999) 269–273.
[59] S. Yang, P. Wang, X. Yang, L. Shan, W. Zhang, X. Shao, R. Niu, Degradation efficiencies of azo dye Acid Orange 7 by the interaction of heat, UV and anions with common oxidants: persulfate, peroxymonosulfate and hydrogen peroxide, J. Hazard. Mater. 179 (1–3) (2010) 552–558, https://doi.org/10.1016/j.jhazmat.2010.03.039.
[60] Y. Zhang, B.J. Wang, K.Y. Fang, Y.Y. Qin, H.J. Li, J. Du, Degradation of p-aminobenzoic acid by peroxymonosulfate and evolution of effluent organic matter: the effect of chloride ion, Chem. Eng. J. 411 (2021), 128462, https://doi.org/10.1016/j.cej.2021.128462.
[61] J.W. Hao, S. Zhao, R. Mao, X. Zhao, Activation of peroxymonosulfate by cobalt doped graphitic carbon nitride for ammonia removal in chloride-containing wastewater, Sep. Purif. Technol. 271 (2021), 118858, https://doi.org/10.1016/j.seppur.2021.118858.
[62] E.A. Betterton, M.R. Hoffmann, Kinetics and Mechanism of the Oxidation of Aqueous Hydrogen-Sulfide by Peroxymonosulfate, Environ. Sci. Technol. 24 (12) (1990) 1819–1824, https://doi.org/10.1021/es00082a005.
[63] G. Lente, J. Kalmar, Z. Baranyai, A. Kun, I. Kek, D. Bajusz, M. Takacs, L. Veres, I. Fabian, One- versus two-electron oxidation with peroxomonosulfate ion: reactions with iron(II), vanadium(IV), halide ions, and photoreaction with cerium (III), Inorg. Chem. 48 (4) (2009) 1763–1773, https://doi.org/10.1021/ic801569k.
[64] J. Ma, H. Li, L. Chi, H. Chen, C. Chen, Changes in activation energy and kinetics of heat-activated persulfate oxidation of phenol in response to changes in pH and temperature, Chemosphere 189 (2017) 86–93, https://doi.org/10.1016/j.chemosphere.2017.09.051.
[65] M. Ahmadi, F. Ghanbari, M. Moradi, Photocatalysis assisted by peroxymonosulfate and persulfate for benzotriazole degradation: effect of pH on sulfate and hydroxyl radicals, Water Sci. Technol. 72 (11) (2015) 2095–2102, https://doi.org/10.2166/wst.2015.437.
[66] P. Neta, R.E. Huie, A.B. Ross, Rate constants for reactions of inorganic radicals in aqueous-solution, J. Phys. Chem. Refer. Data 17 (3) (1988) 1027–1284, https://doi.org/10.1063/1.555808.
[67] Y. Yang, J.J. Pignatello, J. Ma, W.A. Mitch, Comparison of halide impacts on the efficiency of contaminant degradation by sulfate and hydroxyl radical-based advanced oxidation processes (AOPs), Environ. Sci. Technol. 48 (4) (2014) 2344–2351.
[68] M. Moradi, A. Eslami, Reductive/oxidative degradation of tetrachloroethene and its transformation products using combination of permeable ZVI column and UV/Fe/peroxydisulfate system: RSM design and synergy effect study, J. Water Process. Eng. 36 (2020), 101288, https://doi.org/10.1016/j.jwpe.2020.101288.
[69] C.D. Qi, X.T. Liu, C.Y. Lin, H.J. Zhang, X. Li, J. Ma, Activation of peroxymonosulfate by microwave irradiation for degradation of organic contaminants, Chem. Eng. J. 315 (2017) 201–209, https://doi.org/10.1016/j.cej.2017.01.012.
[70] D.L. Ball, J.O. Edwards, The kinetics and mechanism of the decomposition of Caro's acid. I, J. Am. Chem. Soc. 78 (6) (1956) 1125–1129.
[71] S.Y. Yang, Y. Li, L.L. Wang, L.Y. Feng, Use of peroxymonosulfate in wet scrubbing process for efficient odor control, Sep. Purif. Technol. 158 (2016) 80–86, https://doi.org/10.1016/j.seppur.2015.12.010.
[72] X. Lou, L. Wu, Y. Guo, C. Chen, Z. Wang, D. Xiao, C. Fang, J. Liu, J. Zhao, S. Lu, Peroxymonosulfate activation by phosphate anion for organics degradation in water, Chemosphere 117 (2014) 582–585, https://doi.org/10.1016/j.chemosphere.2014.09.046.
[73] F. Yang, Y. Huang, C.L. Fang, Y. Xue, L.Y. Ai, J.S. Liu, Z.H. Wang, Peroxymonosulfate/base process in saline wastewater treatment: the fight between alkalinity and chloride ions, Chemosphere 199 (2018) 84–88, https://doi.org/10.1016/j.chemosphere.2018.02.023.
[74] X.Y. Lou, Y.G. Guo, D.X. Xiao, Z.H. Wang, S.Y. Lu, J.S. Liu, Rapid dye degradation with reactive oxidants generated by chloride-induced peroxymonosulfate activation, Environ. Sci. Pollut. Res. Int. 20 (9) (2013) 6317–6323, https://doi.org/10.1007/s11356-013-1678-x.
[75] G.P. Anipsitakis, D.D. Dionysiou, Radical generation by the interaction of transition metals with common oxidants, Environ. Sci. Technol. 38 (13) (2004) 3705–3712, https://doi.org/10.1021/es035121o.
[76] R. Norman, P. Storey, P. West, Electron spin resonance studies. Part XXV. Reactions of the sulphate radical anion with organic compounds, J. Chem. Soc. B Phys. Organ. (1970) 1087–1095.
[77] Y.F. Ji, C.X. Dong, D.Y. Kong, J.H. Lu, Q.S. Zhou, Heat-activated persulfate oxidation of atrazine: implications for remediation of groundwater contaminated by herbicides, Chem. Eng. J. 263 (2015) 45–54, https://doi.org/10.1016/j.cej.2014.10.097.

[78] C.J. Liang, H.W. Su, Identification of sulfate and hydroxyl radicals in thermally activated persulfate, Ind. Eng. Chem. Res. 48 (11) (2009) 5558–5562, https://doi.org/10.1021/ie9002848.
[79] Y. Gao, Z. Chen, Y. Zhu, T. Li, C. Hu, New insights into the generation of singlet oxygen in the metal-free peroxymonosulfate activation process: Important role of electron-deficient carbon atoms, environmental, Sci. Technol. 54 (2020) 1232–1241, https://doi.org/10.1021/acs.est.9b05856.
[80] Y. Ding, X. Wang, L. Fu, X. Peng, C. Pan, Q. Mao, C. Wang, J. Yan, Nonradicals induced degradation of organic pollutants by peroxydisulfate (PDS) and peroxymonosulfate (PMS): recent advances and perspective, Sci. Total Environ. 765 (2021), 142794, https://doi.org/10.1016/j.scitotenv.2020.142794.
[81] A. Muller, S.C. Weiss, J. Beisswenger, H.G. Leukhardt, W. Schulz, W. Seitz, W. K. Ruck, W.H. Weber, Identification of ozonation by-products of 4- and 5-methyl-1H-benzotriazole during the treatment of surface water to drinking water, Water Res. 46 (3) (2012) 679–690, https://doi.org/10.1016/j.watres.2011.11.033.
[82] G.-.D. Fang, D.D. Dionysiou, Y. Wang, S.R. Al-Abed, D.-.M. Zhou, Sulfate radical-based degradation of polychlorinated biphenyls: effects of chloride ion and reaction kinetics, J. Hazard. Mater. 227-228 (2012) 394–401, https://doi.org/10.1016/j.jhazmat.2012.05.074.
[83] R.X. Yuan, S.N. Ramjaun, Z.H. Wang, J.S. Liu, Photocatalytic degradation and chlorination of azo dye in saline wastewater: kinetics and AOX formation, Chem. Eng. J. 192 (2012) 171–178, https://doi.org/10.1016/j.cej.2012.03.080.
[84] M. Yusuf, Handbook of Textile Effluent Remediation, Pan Stanford, 2018.
[85] C. Fang, D. Xiao, W. Liu, X. Lou, J. Zhou, Z. Wang, J. Liu, Enhanced AOX accumulation and aquatic toxicity during 2,4,6-trichlorophenol degradation in a Co(II)/peroxymonosulfate/Cl(-) system, Chemosphere 144 (2016) 2415–2420, https://doi.org/10.1016/j.chemosphere.2015.11.030.
[86] H. Chaabane, E. Vulliet, F. Joux, F. Lantoine, P. Conan, J.F. Cooper, C.M. Coste, Photodegradation of sulcotrione in various aquatic environments and toxicity of its photoproducts for some marine micro-organisms, Water Res. 41 (8) (2007) 1781–1789, https://doi.org/10.1016/j.watres.2007.01.009.